



Recommended b-Value for Computing Number of Equivalent Stress Cycles and Magnitude Scaling Factors for Simplified Liquefaction Triggering Evaluation Procedures

K. J. Ulmer, A.M.ASCE¹; R. A. Green, F.ASCE²; and A. Rodriguez-Marek, M.ASCE³

Abstract: Magnitude scaling factors (MSFs) account for the influence of ground motion duration on liquefaction triggering in simplified stress-based models in which the duration of the motion is quantified in terms of number of equivalent stress cycles (N_{eq}). Central to computing N_{eq} and MSF is the relationship relating the amplitude of applied loading and the corresponding number of cycles to trigger liquefaction, that is, cyclic stress ratio (CSR)- N_L curves. Based on empirical evidence (and mathematical convenience), CSR- N_L curves are commonly assumed to plot as straight lines on log-log scales, with the line having a slope of -b. As such, the b-value is central to computing N_{eq} and MSF and has a significant influence on computed normalized seismic demand in simplified liquefaction evaluations. It is widely assumed that the b-value varies significantly as a function of soil density. However, in this study a review of published laboratory data and analysis of constant-volume cyclic direct simple shear tests performed as part of this study were used to assess the dependency of the b-value on soil density and other factors. We show that the criterion used to define liquefaction triggering in laboratory tests and the nonlinearity of the CSR- N_L curves can result in the apparent dependency of the b-value on soil density. However, using a consistent liquefaction criterion based on the cumulative dissipated energy in a unit volume of soil yields b-values that are relatively insensitive to changes in soil density. Published modulus reduction and damping (MRD) curves can be used to compute b-values using an energy-based framework; this yields more generalized and less test- and soil-specific b-values. As a result of these efforts, a b-value of 0.28 is recommended for computing N_{eq} and MSF, independent of soil density. **DOI: 10.1061/(ASCE)GT.1943-5606.0002926.** © 2022 American Society of Civil Engineers.

Author keywords: Number of equivalent cycles (N_{eq}) ; Magnitude scaling factor (MSF); Cyclic direct simple shear; Liquefaction evaluation; Dissipated energy.

Introduction

Magnitude scaling factors (MSFs) account for the influence of the duration of ground motion shaking on liquefaction triggering in stress-based simplified models. The basis for MSFs stems from metal fatigue theories wherein loadings of different durations with cycles of varying amplitudes can be converted to an equivalently damaging loading of uniform cycles (i.e., a given number of equivalent cycles having a constant amplitude). Central to this conversion are factors that relate loading characteristics to induced damage. In metal fatigue analyses, this relationship is typically expressed in terms of S-N curves, where S = amplitude of the applied loading, and N = number of cycles to induce failure corresponding to S. Analogously, in liquefaction analyses this relationship is typically expressed in terms of cyclic stress ratio (CSR)- N_L curves,

Note. This manuscript was submitted on June 16, 2021; approved on August 1, 2022; published online on October 8, 2022. Discussion period open until March 8, 2023; separate discussions must be submitted for individual papers. This paper is part of the *Journal of Geotechnical and Geoenvironmental Engineering*, © ASCE, ISSN 1090-0241.

where CSR = amplitude of the applied loading, and N_L = number of cycles required to trigger liquefaction corresponding to CSR. Based on empirical evidence (and mathematical expediency), both S-N and CSR- N_L curves are commonly assumed to plot as straight lines in log-log space, with the line having a slope of -b. However, for both S-N and CSR- N_L curves, the straight-line trend only holds for values of S that exceed the fatigue limit of the metal or for CSR values exceeding the value corresponding to the volumetric threshold strain of the soil.

For historical reasons, MSFs quantify the influence of the duration of shaking on liquefaction relative to the duration of a moment magnitude 7.5 (M7.5) event, where the durations of events having moment magnitudes M and 7.5 are expressed in terms of their corresponding numbers of equivalent stress cycles, N_{eq} and $N_{eq\,M7.5}$, respectively. As noted previously, procedures for computing N_{eq} may also rely on b-values (e.g., Liu et al. 2001; Green and Terri 2005; Hancock and Bommer 2005; Stafford and Bommer 2009; Lasley et al. 2017). For example, if a CSR- N_L curve plots as a straight line in log-log space, then the Seed et al. (1975) procedure for computing N_{eq} can be expressed as

$$N_{eq} = \sum_{i} \left[\left(\frac{a_i}{0.65 \cdot a_{max}} \right)^{\frac{1}{b}} \cdot n_i \right] \tag{1}$$

where $a_i = i$ th amplitude (absolute value) of acceleration pulses in an acceleration time history acting in a horizontal direction recorded at the surface of a soil profile during an earthquake having magnitude M; $n_i =$ number of acceleration pulses in an acceleration time history having amplitude a_i , where i ranges from 1 to the

¹Research Engineer, Geoscience and Engineering Dept., Southwest Research Institute, San Antonio, TX 78238. ORCID: https://orcid.org/0000-0001-8696-7447. Email: kulmer@swri.org

²Professor, Dept. of Civil and Environmental Engineering, Virginia Tech, Blacksburg, VA 24061 (corresponding author). ORCID: https://orcid.org/0000-0002-5648-2331. Email: rugreen@vt.edu

³Professor, Dept. of Civil and Environmental Engineering, Virginia Tech, Blacksburg, VA 24061. ORCID: https://orcid.org/0000-0002-8384-4721. Email: adrianrm@vt.edu

number of different amplitudes of the acceleration pulses in the acceleration time history that are greater than $0.3 \cdot a_{\text{max}}$; and $a_{\text{max}} = \text{maximum}$ value of a_i . Once values for N_{eq} and $N_{eqM7.5}$ are determined, these values can be related to MSF using the following equation:

$$MSF = \left(\frac{N_{eq}}{N_{eqM7.5}}\right)^{-b} \tag{2}$$

As may be surmised from Eqs. (1) and (2), the *b*-value is central to computing MSF and, as such, has a significant influence on computed normalized seismic demand in simplified liquefaction evaluations.

The authors have found general acceptance among practitioners and researchers that the b-value is strongly influenced by the relative density (D_r) of the soil (e.g., Boulanger and Idriss 2014). However, as detailed subsequently in this paper, many factors can affect b-values; often, the influence of these factors is ignored or not fully considered in studies that recommend b-values for liquefaction studies (Ulmer et al. 2018).

The objective of this study was to propose a b-value(s) for computing N_{eq} and MSF for evaluating liquefaction triggering in sandy soils. Toward this end, a critical review of published laboratory data is presented assessing the dependency of the b-value on D_r and other factors, such as the liquefaction triggering criterion used to analyze laboratory data, laboratory testing protocols, and quality acceptance criteria for laboratory data. With regard to quality acceptance criteria, the authors analyzed a large set of constantvolume cyclic direct simple shear (CV-CDSS) tests performed as part of this study. Then, using an alternative approach, the authors interpreted laboratory test data to determine b-values; this was an energy-based approach. This approach was extended to determine b-values using modulus reduction and damping curves, with the derived b-value being more generalized and less test- and soilspecific. The recommended b-value was then compared to other values proposed in the literature. The implications of the recommended value on MSF are also presented and discussed.

Relationship between Relative Density and b-Value

As mentioned previously, the authors found general acceptance among practitioners and researchers that the *b*-value is strongly

influenced by the relative density (D_r) of the soil. As a result, Ulmer et al. (2018) performed a detailed review of data from numerous published laboratory studies to explore the relationships (or lack thereof) between b-values and D_r . The studies that Ulmer et al. (2018) reviewed included cyclic direct simple shear (CDSS), cyclic triaxial (CTRX), and cyclic torsional shear (CTS) test data. The review showed that trends between b-values and D_r are more ambiguous than is widely believed. This is due in part to the nonlinearity in the CSR versus N_L curves in log-log space exhibited by some soils, particularly in the lower value range of N_L for denser soils. If a straight line is fit to all data, an apparent relationship between the b-value and D_r may be observed, with the b-value increasing as D_r increases. However, the b-value for the linear portion of the CSR versus N_L curve is relatively constant for a wide range of D_r values.

For illustration, Fig. 1 displays the results of anisotropically consolidated CTS tests performed by Tatsuoka et al. (1986) on air-pluviated samples of Sengenyama sand. In Fig. 1(a), there is noticeable nonlinearity in the CSR versus N_L curves for samples with $D_r > 60\%$. When a straight line is used to fit all the data, the resulting b-values are larger than those computed only from the linear portion of the curve and increase with increasing D_r . If the b-values are computed only from the linear portions of these curves, as in Fig. 1(b), then the b-values remain relatively constant for D_r ranging from 40% to 90%. The $D_r = 95\%$ group did not have enough data points to identify a linear portion of the CSR versus N_L curve. Similarly, Ulmer et al. (2018) noted that not all testing programs reviewed in their study provided enough data to fully identify the linear and nonlinear portions of CSR versus N_L curves.

Based on their critical review, Ulmer et al. (2018) found that while some data show that b-values increase as D_r increases (as is commonly assumed), other data show that b-values remain constant, decrease, or have no clear trend. However, Ulmer et al. (2018) found that the b-value can be affected by soil type, sample preparation method, effective confining stress, liquefaction triggering criterion, and laboratory testing protocol. In addition, Ulmer et al. (2019) found that quality acceptance criteria of laboratory data also had a significant influence on the b-value. Some of these factors are detailed in the following.

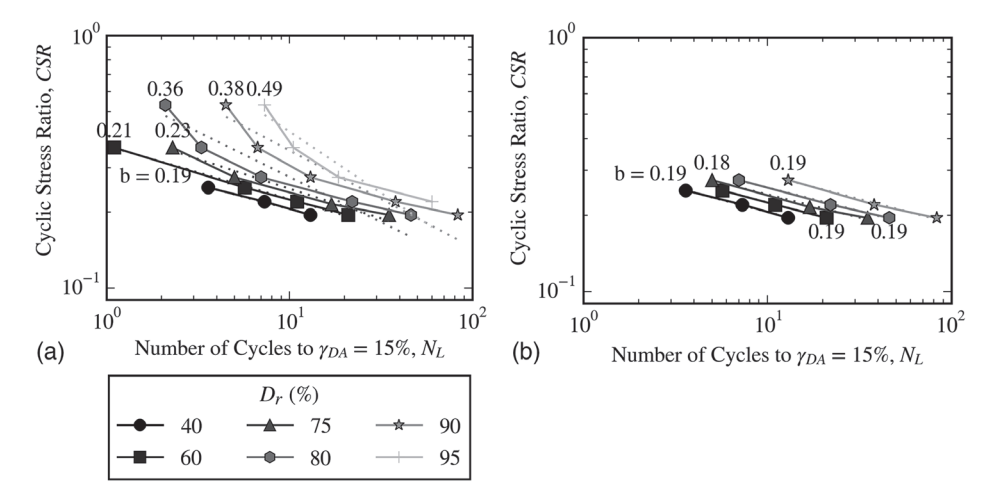


Fig. 1. Anisotropically consolidated CTS tests on air-pluviated samples of Sengenyama sand with *b*-values calculated using (a) all data points; or (b) points on the linear portion of the curve ($\gamma_{DA} = 15\%$). Solid lines represent a spline fit, and dotted lines represent a power law fit. (Data from Tatsuoka et al. 1986.)

Relationship between b-Value and Other Factors

As mentioned previously, there are several factors that can affect the *b*-values computed from tests (Ulmer et al. 2018, 2019). A few of these factors are highlighted in the following.

Effect of Liquefaction Triggering Criteria on b-Values

A liquefaction triggering criterion is required to estimate N_L from cyclic tests, although this criterion is somewhat ambiguous and inconsistent in published studies (Wu et al. 2004). Liquefaction is initiated (or triggered) when the vertical effective stress (σ'_v) reduces to zero (i.e., the complete transfer of the overburden stress to the pore water). This is often expressed in terms of excess pore water pressure ratio (i.e., $r_u = 1$), where r_u is defined as excess pore water pressure, Δu , divided by initial vertical effective stress, σ'_{vo} . However, due to the dilative tendencies of medium-dense to dense soils, $\sigma'_v = 0$ or $r_u = 1$ is not always achievable. As a result, strain-based liquefaction triggering criteria are commonly used, although defining liquefaction triggering in this way entails judgement, particularly for medium dense to dense soils. Common thresholds for CDSS and CTS tests range from 3% to 4% for singleamplitude shear strain (γ_{SA}) and 1.5% to 15% for double-amplitude shear strain (γ_{DA}), and common thresholds for CTRX tests range from 2% to 10% for double-amplitude axial strain (ε_{DA}) (e.g., Tatsuoka and Silver 1981; Tatsuoka et al. 1986; Mandokhail et al. 2017).

In addition to the ambiguity regarding which liquefaction triggering criterion to use to determine N_L , there are also several issues surrounding the most commonly used criteria. For example, ambiguity exists in how the r_u -based criterion is interpreted in determining liquefaction triggering in cyclic tests. As stated previously, liquefaction is unambiguously initiated when $\sigma'_{v} = 0$, which corresponds to $r_u = 1$, but only when the applied loading is zero. In this case, r_u is referred to as residual r_u (i.e., $r_{u,Residual}$) and is the value of r_u in cyclic tests at times when the applied cyclic deviatoric stress (for CTRX tests) or cyclic shear stress (for CDSS or CTS tests) equals zero (i.e., $r_u = r_{u,Residual}$ two times during a loading cycle for a specimen that does not have an imposed static stress). In lieu of using $r_{u,Residual} = 1$ to define liquefaction, $r_{u,Transient} = 1$ is often used, where $r_{u,\text{Transient}} = r_u$ at any time during a cycle of loading; note that $r_{u,\text{Transient}} = 1$ does not necessarily correspond to $\sigma'_v = 0$. It is likely that most published studies that purport to define

liquefaction as $r_u = 1$ are defining it as $r_{u,Transient} = 1.0$, unless it is explicitly stated that $r_{u,Residual} = 1.0$ is used as the liquefaction triggering criterion. The reason for this is that dense sands and silty sands often stop accumulating excess pore pressure before reaching $r_{u,\text{Residual}} = 1.0$, despite accumulating large strains during cyclic loading—but they may reach a state where $r_{u,\text{Transient}} = 1$ (Wu et al. 2004). Also, pore pressures in a soil specimen during a cyclic test can be somewhat difficult to measure accurately, particularly when excess pore pressures do not rapidly and evenly distribute throughout the soil specimen—for example, in silty sands (Casagrande 1976; Wu et al. 2004). Regarding strain-based triggering criteria, the value of N_I in medium-dense to dense sands can be very sensitive to the assumed strain threshold, while the value for loose sands is not as sensitive (Wu et al. 2004; El Mohtar 2009). Given that judgement is used in selecting the strain threshold, the value of N_L for medium-dense to dense sands is inherently subjective.

To illustrate the effect of liquefaction triggering criterion, b-values and the associated standard errors (ϵ_b) were computed using published data from a number of studies in which CTRX, CDSS, and CTS tests were performed (Ulmer et al. 2018). A large ϵ_b indicates a high degree of uncertainty in the associated b-value, which may result from a CSR versus N_L curve that is not linear in log-log space, significant scatter in the test data, and/or the available data representing a small range of N_L . In general, increasing the threshold value of a given liquefaction criterion or changing the criterion from one type (e.g., based on r_u) to another (e.g., based on strain) has an effect on the b-value and should be considered when determining b-values. For example, Fig. 2 shows that b-values from $r_{u,Residual}$ -based criteria can be significantly different from b-values from strain-based criteria. These differences are more pronounced in denser sands than in looser sands. Furthermore, Fig. 3 shows that sample preparation method can have varying influences on b-values determined using different liquefaction triggering criteria. If samples were prepared using air pluviation, then b-values were less affected by the choice of $\varepsilon_{\mathrm{DA}}$ than if the samples were prepared using wet vibration.

Effect of Testing Protocol on b-Values

The influence of testing protocol on *b*-values is illustrated by the results of a cooperative testing program that involved multiple laboratories performing CTRX tests on reconstituted samples from the

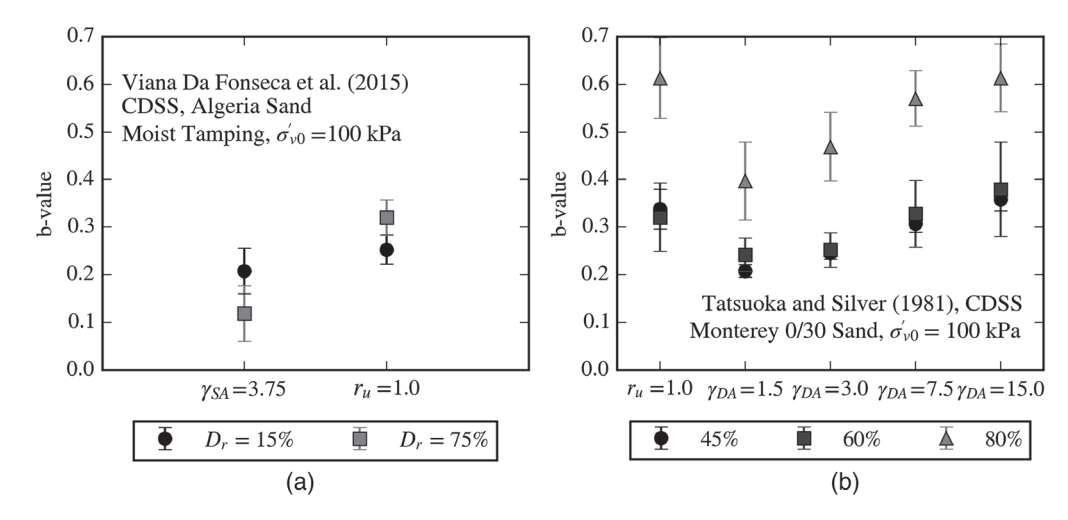


Fig. 2. Effects of liquefaction triggering criteria on b-values from CDSS tests on clean sands from two studies: (a) Viana Da Fonseca et al. (2015); and (b) Tatsuoka and Silver (1981). Error bars represent +/- standard error, ϵ_b . Note: r_u is assumed to represent $r_{u,\text{Residual}}$ in these studies.

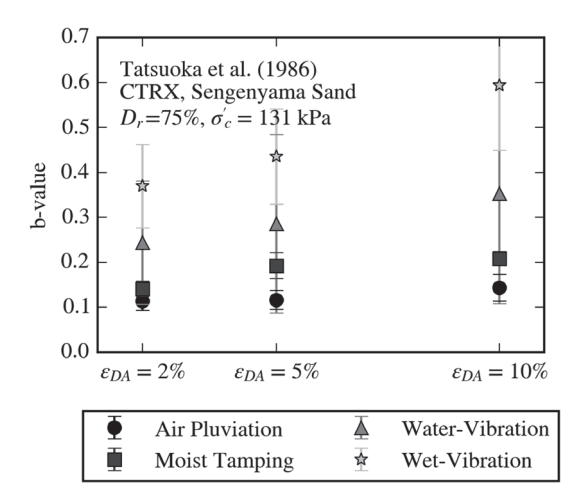


Fig. 3. Effects of liquefaction triggering criteria on *b*-values from CTRX tests on clean sands. Error bars represent +/- standard error, ϵ_b . (Data from Tatsuoka et al. 1986.)

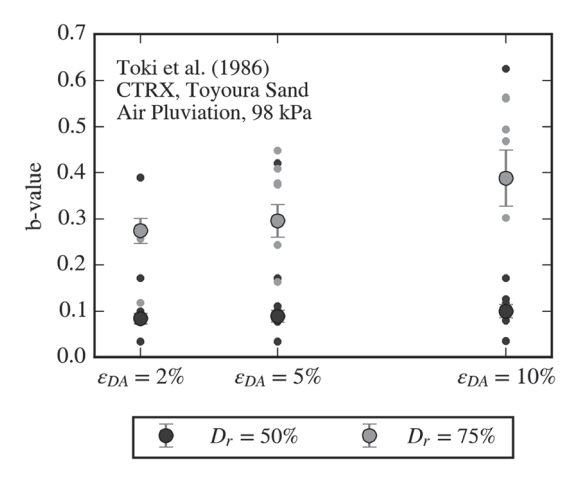


Fig. 4. Range of *b*-values from multiple laboratories that performed the same test on the same sand. Dots represent *b*-values from individual laboratories, while larger symbols and error bars represent the *b*-value and +/— standard error of the mean resulting from the data combined from all laboratories. (Data from Toki et al. 1986.)

same batch of Toyoura sand (Toki et al. 1986). As shown in Fig. 4, the results from this study yielded a range of b-values from the various laboratories, presumably due to differences in the testing protocols among the laboratories. While we did not attempt to assess the appropriateness of the testing protocols used by the various laboratories, it was clear that differences in operators, apparatuses, specimen dimensions, and potentially other unidentified factors likely affected the b-values. Note that the data in this figure also illustrate the influence of the liquefaction triggering criterion on the b-value, with the spread of the individual b-values increasing as the value of the $\varepsilon_{\mathrm{DA}}$ used to define liquefaction initiation increased.

Effect of Test Quality Acceptance Criterion on b-Values

To examine how quality acceptance criteria for laboratory test data can affect *b*-values, Ulmer et al. (2019) performed a series of CV-CDSS tests on Monterey 0/30 sand specimens (the Supplemental Materials provide additional details regarding this testing). Monterey 0/30 sand is poorly graded clean sand with subangular to

Table 1. Index properties of Monterey 0/30 sand

Minimum void ratio, e_{\min}	0.562
Maximum void ratio, e_{max}	0.827
Specific gravity of solids, G_s (assumed)	2.66
Minimum mass density, ρ_{min} (g/cm ³)	1.46
Maximum mass density, ρ_{max} (g/cm ³)	1.70
$D_{60}^{a} \text{ (mm)}$	0.595
$D_{50}^{a} \text{ (mm)}$	0.545
$D_{30}^{a} \text{ (mm)}$	0.450
$D_{10}^{a} \text{ (mm)}$	0.330
Coefficient of curvature, C_c	1.03
Coefficient of uniformity, C_u	1.80

^aFor each D_x , x% of the soil (by weight) is finer than D_x .

rounded particles. The index properties and grain-size distribution of this sand are shown in Table 1 and Fig. 5, respectively. The specimens were prepared using air pluviation (Vaid and Negussey 1988) to different D_r values and confined to σ'_{vo} values of 60, 100, or 250 kPa. The specimens were subjected to stress-controlled, sinusoidal horizontal loading at their bases, having a predetermined CSR. The tests performed by Ulmer et al. (2019) maintained constant volume during the cyclic phase using passive control (PC). PC maintains constant volume via a physical locking mechanism designed to minimize axial deformation. The cyclic phase of the tests continued until the horizontal linear variable differential transformer (LVDT) reached its limit, and liquefaction initiation was defined as $\gamma_{\rm SA}=3.5\%$.

Ulmer et al. (2019) developed and applied acceptance criteria for the PC CV-CDSS tests. The criteria included acceptable levels of shear stress (τ) and shear strain (γ) during consolidation (i.e., prior to cyclic loading), acceptable levels of axial strain (ε) during the cyclic loading phase, and the presence of several anomalies in the τ versus σ'_v path (see Supplemental Materials). For each criterion, a grade of A-D was assigned, and each grade was associated with a numerical score (Table 2). Tests that earned a grade of D in any of the categories or that manifested irregular spacing or a bias in the τ versus σ'_{ν} path (i.e., asymmetrical shape in the stress paths around $\tau = 0$) were automatically excluded. For each remaining test, a total score was then computed as the sum of all numerical scores associated with the letter grades. It was observed, however, that soil samples with $D_r = 25\%$ were able to achieve higher scores more easily than samples with $D_r = 60\%$ or 80% (the maximum possible score was 10; a very low score was lower than -1). Therefore, the minimum total scores for the quality acceptance criteria were adjusted based on D_r values of 8.5, 8.0, and 6.5 for D_r = 25%, 60%, and 80%, respectively, in order to have sufficient tests in each D_r bin. Note that all test data that passed the quality acceptance threshold scores and many of the tests that did not would almost assuredly have been included in previously published studies (i.e., the use of the threshold quality acceptance criteria proposed herein results in an exceptionally high-quality test data set).

To investigate the effect of removing tests that did not pass the PC CV-CDSS quality acceptance criteria, with focus on $\sigma'_{vo}=100$ kPa and using $\gamma_{\rm SA}=3.5\%$ to define liquefaction, Ulmer et al. (2019) computed the *b*-values for two scenarios: (1) only tests that passed the acceptance criteria and met the minimum total score were included; and (2) a random sample of all tests was selected. The random sample included the number of cyclic tests performed for a typical liquefaction resistance study (e.g., 4 to 5 tests). The *b*-values using only those tests that passed the acceptance criteria were 0.17, 0.16, and 0.19 for $D_r=25\%$, 60%, and 80%, respectively. The *b*-values obtained using 1,000 random samples of 4 to 5 tests from the entire data set (i.e., all available data for tests

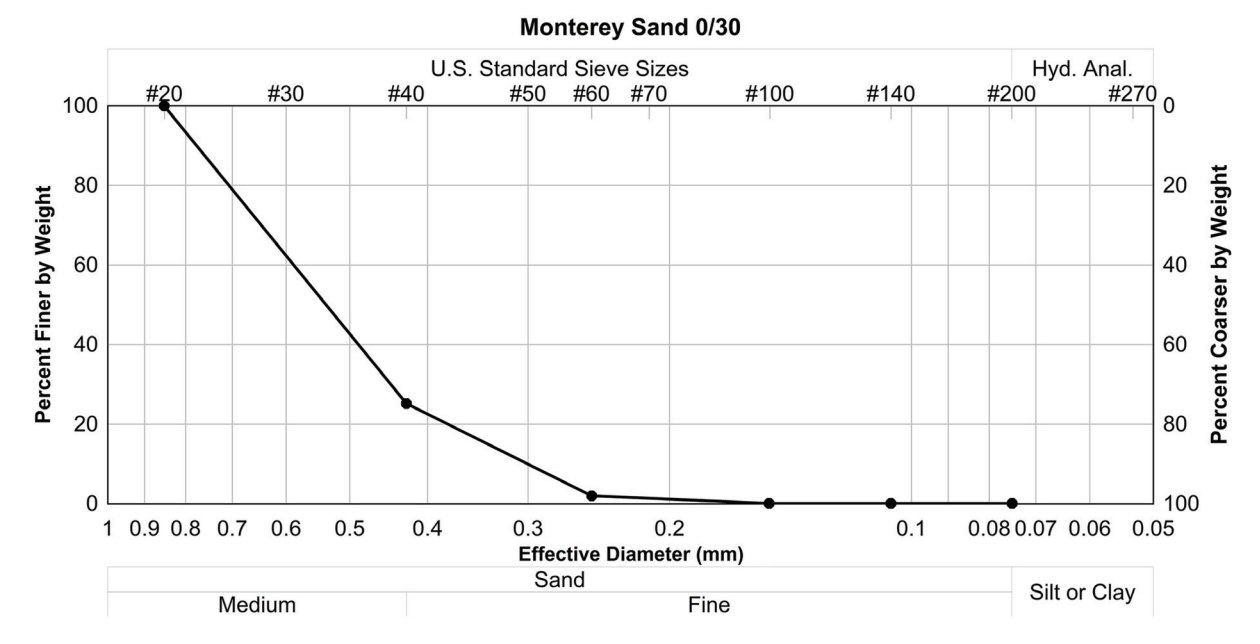


Fig. 5. Grain-size distribution of Monterey 0/30 sand.

Table 2. Quality acceptance criteria for PC CV-CDSS tests

Criterion	A–D	Score ^a
γ during ramp-up, consolidation		
$\gamma \le 0.05\%$	A	+3
$\gamma \leq 0.10\%$	В	+2
$\gamma \le 0.20\%$	C	+1
$\gamma > 0.20\%$	D	_
au during ramp-up, consolidation		
$\tau \le 1.0 \text{ kPa}$	A	+3
$\tau \le 2.0 \text{ kPa}$	В	+2
$\tau \le 3.0 \text{ kPa}$	C	+1
$\tau > 3.0 \text{ kPa}$	D	_
ε during cyclic phase (c.p.)		
$\varepsilon \le 0.05\%$ for 80% of the c.p.	Α	+3
or until $r_u = 0.75$		
$\varepsilon \le 0.05\%$ for 60% of the c.p.	A-	+2.5
$\varepsilon \le 0.05\%$ for 40% of the c.p.	$\mathrm{B}+$	+2
$\varepsilon \le 0.10\%$ for 100% of the c.p.	В	+1.5
or until $r_u = 0.75$		
$\varepsilon \le 0.10\%$ for 75% of the c.p.	B-	+1
$\varepsilon \le 0.10\%$ for 50% of the c.p.	C	+0.5
$\varepsilon > 0.10\%$ within 50% of the c.p.	D	_
Vertical line in τ versus σ'_v path		
There is a vertical line	True	-1
	False	+1
Stress path convergence		
Converges to $\sigma'_v = \sigma'_{\min} > 0$	True False	$-10 \times \left(\sigma_{\min}'/\sigma_{vo}'\right)$

^aModification for AC tests: AC tests with a bias in the τ versus σ'_v path (i.e., asymmetrical shape in the stress paths around $\tau = 0$) received a reduction in their total score of -1, whereas tests that did not have this bias received an increase in their total score of +1.

having $\sigma'_{vo}=100$ kPa, including those which did not pass the new acceptance criteria but which may have generally been acceptable in other studies) for each D_r ranged from 0.05 to 0.65, 0.02 to 0.39, and 0.09 to 0.31 for $D_r=25\%$, 60%, and 80%, respectively. This shows that the use of the quality acceptance criteria affected the possible range of b-values, particularly when only a few tests were performed for a given D_r .

In addition to the PC CV-CDSS tests performed by Ulmer et al. (2019), the authors also performed a series of active control (AC) CV-CDSS tests as part of the present study (the Supplemental Materials provide additional details about this testing). These tests were also performed using Monterey 0/30 sand specimens prepared using air pluviation to different D_r values and confined to σ'_{vo} values of 60, 100, or 250 kPa. AC uses a feedback loop between the vertical actuator and an LVDT close to the top of the specimen to reduce vertical deformations (generally, axial strains were within $\pm 0.05\%$ before liquefaction initiated). A similar set of quality acceptance criteria to those chosen for the PC CV-CDSS tests (Table 2), with a few modifications, was developed as part of the present study and applied to the AC CV-CDSS tests. Because the AC CV-CDSS tests used an active feedback loop to maintain constant volume, the axial strains were more effectively restricted than they would have been by using physical means (e.g., PC); for nearly all of the AC tests, ε was less than 0.05% during the cyclic phase. Therefore, the AC tests achieved higher total scores in general, and the minimum acceptable total scores adopted for the PC tests did not result in the exclusion of many of the AC tests due to excessive vertical strains. However, the presence of a biased τ versus σ'_v path (i.e., asymmetrical shape in the stress paths around $\tau = 0$) was more prevalent in the AC tests than in the PC tests. AC tests with a bias in the τ versus σ'_v path were allowed but received a reduction in their total score of -1. Tests that did not have this bias received an increase in their total score of +1. Each test was assessed using the acceptance criteria, and a sensitivity analysis was performed to identify the minimum total score below which the b-values would be noticeably influenced.

When developing the quality acceptance criteria for the PC tests, the focus was on tests performed with $\sigma'_{vo}=100$ kPa, because there were relatively few tests performed with $\sigma'_{vo}=60$ and 250 kPa. Therefore, the minimum threshold scores for the PC tests were not dependent on σ'_{vo} . When developing the quality acceptance criteria for the AC tests performed as part of the present study, sufficient AC tests were performed with $\sigma'_{vo}=60$ and 250 kPa to observe a relationship between the mean total score and initial vertical effective confining stress. Tests performed with $\sigma'_{vo}=250$ kPa tended to be more prone to slightly higher values of

au during the ramp-up and consolidation stages and more often had a biased au versus σ'_v path. Both of these tendencies led to a lower mean total score. However, D_r did not have a significant effect on the total scores of the AC tests, mainly because the AC method was better able to maintain constant volume conditions (an issue for high D_r samples in PC tests). Therefore, the identified minimum acceptable scores for the AC CV-CDSS tests were not dependent on D_r but were dependent on σ'_{vo} and were assigned as 7.0, 7.0, and 6.0 for $\sigma'_{vo}=60$, 100, and 250 kPa, respectively, for all D_r values. Applying this screening criterion resulted in the removal of approximately 20% of the AC CV-CDSS tests.

Using the AC CV-CDSS tests that passed the acceptance criteria and had a minimum total score of 10.0, the b-values were 0.19, 0.29, and 0.36 for $D_r = 25\%$, 60%, and 80%, respectively ($\sigma'_{vo} =$ 100 kPa, $\gamma_{SA} = 3.5\%$). The b-values obtained using 1,000 random samples of four tests from the entire data set for each D_r ranged from 0.12 to 0.32, 0.08 to 0.40, and 0.22 to 0.71 for $D_r = 25\%$, 60%, and 80%, respectively. Note that the four random tests were selected such that they were not clustered around a narrow range of N_L values to produce erroneous b-values (i.e., two of the four tests had N_L values less than the mean value of N_L , and two had N_L values greater than the mean value of N_L). The minimum difference between maximum and minimum N_L values from any single iteration was seven cycles. Again, as with PC CV-CDSS tests, the use of acceptance criteria affected the possible range of b-values for AC CV-CDSS tests, particularly when only a few tests were performed for a given D_r .

Alternative Approach to *b*-Value Determination: Dissipated Energy

So far, it is clear that there is significant uncertainty in b-values determined using the foregoing approaches, due in large part to the selection of a liquefaction triggering criterion and the quality acceptance criteria of laboratory tests. It is also clear that a consistent liquefaction criterion to apply to laboratory tests that results in more confident estimates of b-values is desirable. Toward this end, the authors propose the use of an energy-based criterion, as detailed in the following.

Justification for Using Dissipated Energy

The basis for using energy-based liquefaction triggering criteria is the relationship between dissipated energy in a unit volume of soil and the generation of excess pore pressures leading to liquefaction (Nemat-Nasser and Shokooh 1979; Green et al. 2000; Polito et al. 2008). Energy is primarily dissipated in sands due to friction developed from relative movement between sand grains as the soil skeleton breaks down under cyclic loading. In addition, dissipated energy underlies the commonly used approaches to compute N_{eq} for earthquake motions, whether explicitly (e.g., Green and Terri 2005; Lasley et al. 2017) or implicitly (e.g., Seed et al. 1975; Boulanger and Idriss 2015). These fundamental relationships make a strong case for using an energy-based criterion to identify liquefaction initiation in laboratory tests and thereby define b-values.

Dissipated energy in a unit volume of soil (ΔW) in laboratory tests is the cumulative area bound by shear stress–shear strain hysteresis loops, such as those shown in Fig. 6, and can be computed using the trapezoidal rule (Green 2001):

$$\Delta W = \frac{1}{2} \sum_{k=1}^{n-1} (\tau_{k+1} + \tau_k) (\gamma_{k+1} - \gamma_k)$$
 (3)

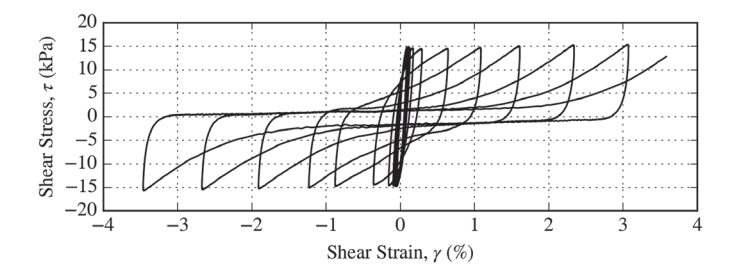


Fig. 6. Shear stress–strain hysteresis loops of a CDSS test on Monterey 0/30 sand ($D_r = 62\%$, CSR = 0.156, $\sigma'_{vo} = 100$ kPa).

where $\tau_k = k$ th increment of shear stress; $\gamma_k = k$ th increment of shear strain (in decimal form); and n = total number of digitized points in the shear stress and shear strain time histories. A threshold value of ΔW can be used to designate when liquefaction initiates during a laboratory test, just as threshold values for shear strain, axial strain, $r_{u,\text{Residual}}$, or $r_{u,\text{Transient}}$ can be used. To account for variations in σ'_{vo} , the energy-based threshold is defined as a normalized value, $\Delta W/\sigma'_{vo}$.

In both laboratory tests and appropriate numerical analyses, normalized dissipated energy (i.e., $\Delta W/\sigma'_{vo}$) can be determined within either an effective stress or a total stress framework; an effective stress framework includes the influence of the reduction in soil stiffness on energy dissipation due to excess pore water pressures, and a total stress framework does not. Inherently, computing $\Delta W/\sigma'_{vo}$ by directly integrating the shear stress–shear strain hysteresis loops from CV-CDSS laboratory tests (e.g., Fig. 6) results in a value of dissipated energy that includes the influence of the reduction in soil stiffness due to excess pore water pressures (i.e., $\Delta W_{eff}/\sigma'_{vo}$). This is indicated by the increased size of the hysteresis loops due to excess pore water pressure generation as cyclic loading progresses. However, in the early phases of loading, the hysteresis loops are relatively constant in shape; the size of the loops increases in later phases of loading as excess pore water pressures increase. This is illustrated by the constant slope of $\Delta W_{eff}/\sigma'_{vo}$ from a CV-CDSS test plotted as a function of the number of cycles of applied loading (N_{cyc}) (e.g., Fig. 7), where $\Delta W_{eff}/\sigma'_{vo}$ is plotted every half-cycle of loading at times when the applied shear stress is equal to zero (i.e., $\tau=0$). The influence of the reduction in soil stiffness due to excess pore water pressures results in the plot of $\Delta W_{eff}/\sigma'_{vo}$ versus N_{cyc} deviating from a straight line; this occurred at approximately 6.5 cycles for the CV-CDSS test data shown in Fig. 7.

Based on the trends illustrated in Fig. 7, the influence of the reduction in soil stiffness due to excess pore water pressures on dissipated energy can be removed by extrapolating the straight-line

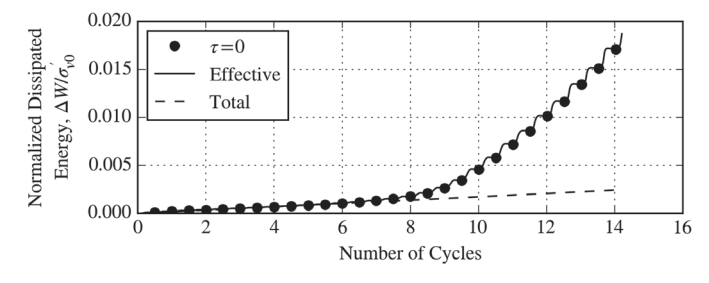


Fig. 7. Illustration of effective and total normalized dissipated energy $(\Delta W_{eff}/\sigma'_{vo})$ and $\Delta W_{total}/\sigma'_{vo}$, respectively) for the same CDSS test on Monterey 0/30 sand represented in Fig. 6.

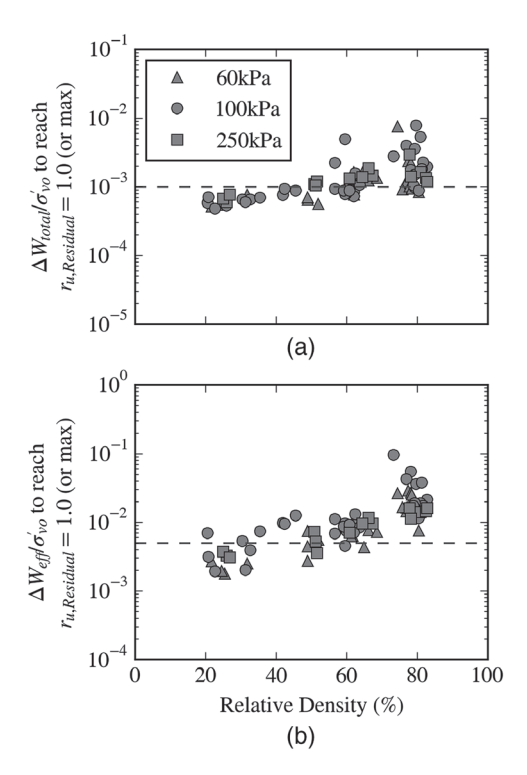


Fig. 8. Relationship between D_r for CV-CDSS tests performed in this study: (a) $\Delta W_{\rm total}/\sigma'_{vo}$ to reach $r_{\rm u,Residual}=1.0$ (or its maximum value); and (b) $\Delta W_{eff}/\sigma'_{vo}$ to reach $r_{\rm u,Residual}=1.0$ (or its maximum value).

portion of the plot of $\Delta W_{eff}/\sigma'_{vo}$ versus N_{cyc} from the early phase of loading to the later phase of loading. This is illustrated in Fig. 7; the extrapolated line represents $\Delta W/\sigma'_{vo}$ determined within a total stress framework (i.e., $\Delta W_{\rm total}/\sigma'_{vo}$). Note that $\Delta W_{\rm total}/\sigma'_{vo}$ is comparable to values of $\Delta W/\sigma'_{vo}$ determined using equivalent-linear site response analyses where damping and shear modulus remain unchanged throughout the application of the loading time history (Green 2001). Threshold values of $\Delta W_{eff}/\sigma'_{vo}$ or $\Delta W_{\rm total}/\sigma'_{vo}$ can be used to define the initiation of liquefaction in a laboratory test, with the corresponding value of N_{cyc} being designated as N_L . The threshold value of $\Delta W_{\rm total}/\sigma'_{vo}$ or $\Delta W_{eff}/\sigma'_{vo}$ used as the

liquefaction triggering criterion is somewhat subjective (similar to selecting a threshold value of shear or axial strain), but $\Delta W_{\rm total}/\sigma'_{vo}=0.001$ or $\Delta W_{eff}/\sigma'_{vo}=0.005$ were used herein because they are closely associated with the point at which $r_{u,\rm Residual}$ reached 1.0 or its maximum value in the tests, as shown in Fig. 8.

The b-Values from AC CV-CDSS Tests

The AC CV-CDSS tests performed as part of this study that met the quality acceptance criteria (Table 2) and met the minimum scores (7.0, 7.0, and 6.0 for $\sigma'_{vo}=60$, 100, and 250 kPa, respectively) were analyzed using the energy-based criteria. The value of N_L was estimated for each test, and b-values were computed using a best-fit regression of the data using a power-law function (i.e., a straight line in log-log space). The value of ϵ_b was also obtained as part of the curve-fitting algorithm and represents the uncertainty in the b-values.

Fig. 9 shows the relationship between b-values (with error bars representing $\pm \epsilon_b$) and D_r using the energy-based criteria of $\Delta W_{\rm total}/\sigma'_{vo}=0.001$ and $\Delta W_{eff}/\sigma'_{vo}=0.005$. Only AC CV-CDSS tests that passed the quality acceptance criteria set forth in Table 2 were included in this figure (the Supplemental Materials provide additional details about these tests). The figure shows that, in general, b-values were relatively constant with increasing D_r when $\Delta W_{\text{total}}/\sigma'_{vo} = 0.001$ was used as the liquefaction triggering criterion; they were a little less so when $\Delta W_{eff}/\sigma'_{vo} = 0.005$ was used. In addition, the b-values were relatively insensitive to the selection of the threshold value of $\Delta W_{\text{total}}/\sigma'_{vo}$ to define liquefaction, as long as the selected $\Delta W_{\rm total}/\sigma'_{vo}$ threshold values were reasonable. For comparison purposes, the same test data were analyzed using more traditional liquefaction triggering criteria, $\gamma_{SA} = 3.5\%$ and $r_{u.\text{Residual}} = 0.98$. These latter results are plotted in Fig. 10 and show increasing b-values as D_r increases, consistent with some previous studies and inconsistent with other previous studies. Comparing the plots in Figs. 9 and 10 highlights how much more stable the b-values were when the energy-based criteria were used.

The b-Values from Modulus Reduction and Damping Curves

Up to this point in the paper, soil-specific *b*-values derived from cyclic laboratory tests have been the focus of the discussion. However, it is also possible to compute *b*-values that are not linked

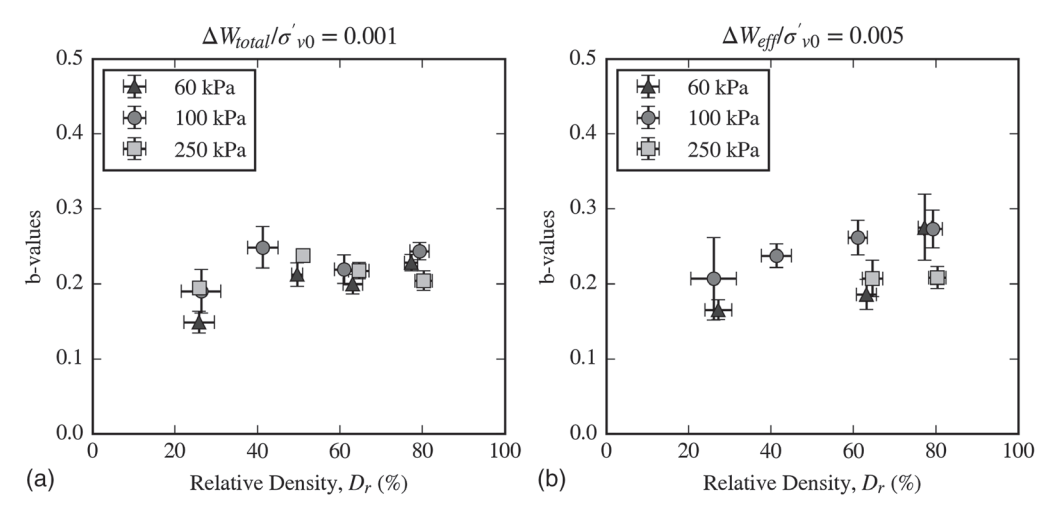


Fig. 9. Relationship between *b*-values and D_r for two energy-based liquefaction triggering criteria in AC CV-CDSS tests on Monterey 0/30 sand: (a) $\Delta W_{\text{total}}/\sigma'_{vo} = 0.001$; and (b) $\Delta W_{eff}/\sigma'_{vo} = 0.005$. Error bars represent +/- standard error, ϵ_b .

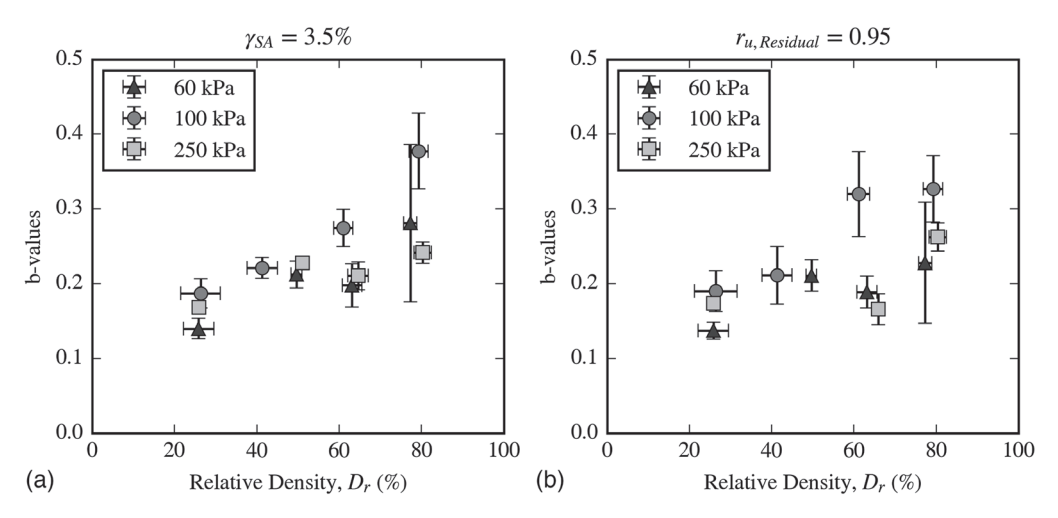


Fig. 10. Relationship between b-values and D_r for two traditionally used liquefaction triggering criteria in AC CV-CDSS tests on Monterey 0/30 sand: (a) $\gamma_{\rm SA} = 3.5\%$; and (b) $r_{u,\rm Residual} = 0.95$. Error bars represent +/- standard error, ϵ_b .

to a specific soil by using contours of constant dissipated energy computed using modulus reduction and damping (MRD) curves, as mentioned in Green et al. (2019). Assuming that the relationship between CSR and N_L is a contour of constant dissipated energy, the b-value representing this relationship can be computed by estimating CSR for a range of N_L values from the dissipated energy per unit volume of soil for a M7.5 event ($\Delta W_{M7.5}$). Toward this end, the same approach used in equivalent-linear site response analysis can be used to compute $\Delta W_{M7.5}$: using a viscoelastic constitutive model in conjunction with MRD curves (e.g., Ishibashi and Zhang 1993; Darendeli 2001). This approach is represented with the following equation:

$$\Delta W_{M7.5} = \frac{2\pi D_{\gamma} (CRR_{M7.5} \cdot K_{\gamma} \cdot \sigma'_{vo})^2}{G_{max} (\frac{G}{G_{max}})_{\gamma}} N_{eq M7.5} \tag{4}$$

where $N_{eqM7.5}$ is assumed to be 14 cycles (e.g., Green et al. 2019), per Approach 2 of Lasley et al. (2017) for shallow crustal events in active tectonic regimes (e.g., western US), where Approach 2 accounts for both horizontal components of motion; $CRR_{M7.5}$ is the cyclic resistance ratio normalized to the shaking duration of a M7.5 event determined from a liquefaction triggering curve (e.g., Green et al. 2019); K_{γ} accounts for the overburden per Green et al. (2022) and is analogous to the overburden correction factor, K_{σ} ; G_{\max} is the small-strain shear modulus; and D_{γ} and $(G/G_{\max})_{\gamma}$ are the damping and shear modulus ratios, respectively, associated with a given value of γ .

Because the relationship between CSR versus N_L is assumed to be a contour of constant dissipated energy, the remaining portions of the curve can be computed for different amplitudes of loading (i.e., CSR) by simply computing the number of cycles for the assumed loading amplitude required for the dissipated energy to equal $\Delta W_{M7.5}$. In this approach, the ΔW for one cycle of loading (i.e., ΔW_1) having amplitude CSR is computed as:

$$\Delta W_1 = \frac{2\pi D_{\gamma} (CSR \cdot \sigma'_{vo})^2}{G_{max} (\frac{G}{G_{max}})_{\gamma}}$$
 (5)

and the N_L corresponding to this CSR amplitude is $\Delta W_{M7.5}/\Delta W_1$. Note that in this approach for determining the CSR versus N_L curve, $\Delta W_{M7.5}$ and ΔW_1 are analogous to total dissipated energy $(\Delta W_{\text{total}})$ in laboratory tests. Once the CSR versus N_L curve that

represents a contour of constant dissipated energy is developed, the b-value is estimated following the same approach as is used in determining the b-value from laboratory test data, using a power-law function to fit the CSR versus N_L relationship.

To estimate $\Delta W_{M7.5}$ and ΔW_1 , $G_{\rm max}$ is computed as $G_{\rm max} = \rho V_s^2$ where ρ is mass density of the soil and V_s is small-strain shear-wave velocity. The value of ρ can be reasonably assumed to be 1,988.45 kg/m³ (19.5 kN/m³, e.g., Moss et al. 2006; Green et al. 2014), and V_s can be estimated from normalized cone tip resistance from the cone penetration test (CPT) corrected for fines, q_{c1Ncs} (Boulanger and Idriss 2014), using a correlation developed by Ulmer et al. (2020) specifically for liquefaction evaluations:

$$V_s = 16.88 (q_{c1Ncs})^{0.489} \left(\frac{\sigma'_{vo}}{P_a}\right)^{0.25} \tag{6}$$

where P_a is atmospheric pressure in the same units as σ'_{vo} . Although an estimate of V_s (or G_{\max}) is necessary to compute $\Delta W_{M7.5}$ or ΔW_1 individually, it appears in both the numerator and the denominator when computing $N_L = \Delta W_{M7.5}/\Delta W_1$, and it is cancelled out. Therefore, the value of N_L (and b-value, as will be shown subsequently) computed from MRD curves in this manner is not contingent on the chosen V_s or G_{\max} correlation.

Values of D_{γ} and $(G/G_{\rm max})_{\gamma}$ can be determined using any published, applicable MRD curves. In this study, both the Ishibashi and Zhang (1993) and Darendeli and Stokoe (Darendeli 2001) curves are used, hereafter denoted IZ and DS, respectively. These MRD curves are dependent on the initial mean effective stress, σ'_{mo} , and soil type or plasticity index, PI. For the purposes of this study, PI was assumed to equal zero and σ'_{mo} was computed as a function of the at-rest lateral earth pressure coefficient, K_o , which is assumed to equal 0.5. Fig. 11 shows an example set of CSR versus N_L curves developed using this method in conjunction with the IZ MRD curves.

Using this procedure, b-values were regressed for a range of q_{c1Ncs} and σ'_{vo} values (Table 3; additional details provided in Table S2). Values of q_{c1Ncs} were correlated to D_r using the following expression (Salgado et al. 1997a, b; Idriss and Boulanger 2008):

$$D_r = 0.478(q_{c1Ncs})^{0.264} - 1.063 (7)$$

where D_r is in decimal. These same b-values are plotted as a function of D_r in Fig. 12 along with the b-values from the AC

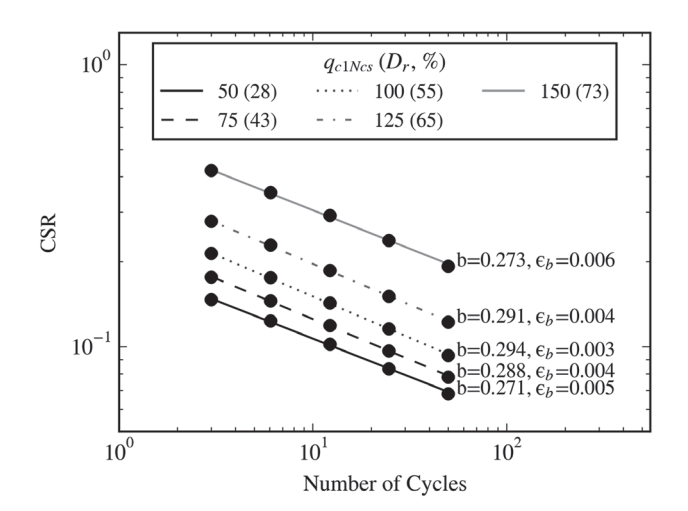


Fig. 11. CSR versus N_L trends developed from IZ MRD curves $(\sigma'_{vo}=100 \text{ kPa} \text{ and } K_o=0.5).$

Table 3. Summary of *b*-values for different combinations of q_{c1Ncs} , σ'_{vo} , and MRD curves

			b-values			
q_{c1Ncs}	D_r (%)	σ'_{vo} (kPa)	IZ	ϵ_b	DS	ϵ_b
50	28	60	0.26	0.006	0.19	0.007
75	43	60	0.27	0.004	0.22	0.007
100	55	60	0.28	0.003	0.23	0.006
125	65	60	0.28	0.004	0.23	0.007
150	73	60	0.26	0.006	0.19	0.007
50	28	100	0.27	0.005	0.19	0.008
75	43	100	0.29	0.004	0.22	0.007
100	55	100	0.29	0.003	0.23	0.007
125	65	100	0.29	0.004	0.23	0.007
150	73	100	0.27	0.006	0.19	0.008
50	28	250	0.29	0.006	0.18	0.007
75	43	250	0.31	0.005	0.21	0.008
100	55	250	0.31	0.004	0.23	0.007
125	65	250	0.31	0.004	0.22	0.006
150	73	250	0.29	0.006	0.18	0.007

Note: IZ = Ishibashi and Zhang (1993); and DS = Darendeli (2001).

CV-CDSS tests shown previously using energy-based liquefaction triggering criteria: $\Delta W_{\rm total}/\sigma'_{vo}=0.001$. In general, b-values remain relatively constant with increasing D_r and σ'_{vo} . The b-values computed using IZ MRD curves are higher than the b-values from using the DS MRD curves for all combinations of D_r and σ'_{vo} .

Although either of the two MRD curves used in this study (among others) could be used to estimate b-values, the authors prefer the IZ MRD curves because they are valid for the full range of shear strains of interest and have been shown to yield consistent trends with liquefaction test data (Green et al. 2022). An average b-value from the IZ MRD curves for $\sigma'_{vo} = 100$ kPa is 0.28. Note that although the b-values showed some sensitivity to changes in D_r and σ'_{vo} , the ranges of b-values from the IZ and DS MRD curves shown in this study (IZ: 0.25-0.31; DS: 0.18-0.23) have only a mild impact on MSF. Finally, it is noted that although the range of b-values for the DS MRD curves better match the b-values from the laboratory tests performed as part of this study, the range of b-values for the IZ MRD curves better represent the range from laboratory tests presented in literature for varying soils, test conditions, etc.

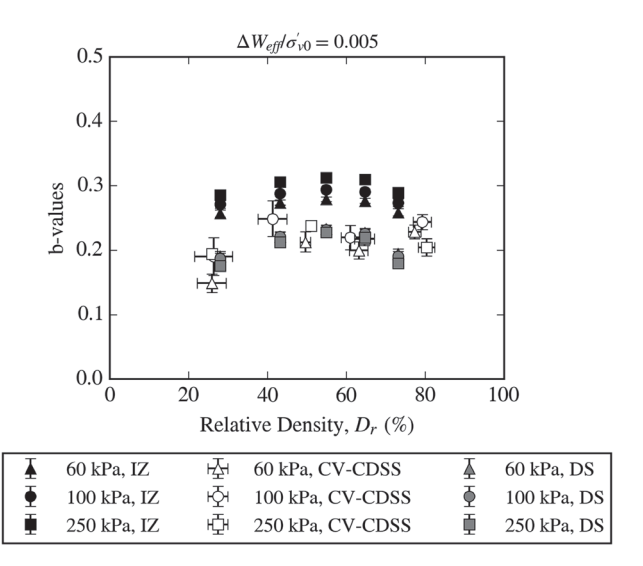


Fig. 12. Relationship between b-values and D_r for AC CV-CDSS laboratory tests using $\Delta W_{\rm total}/\sigma'_{vo}=0.001$ as the liquefaction triggering criterion (white markers) compared to b-values computed from the IZ and DS MRD curves (filled-in markers) for a range of initial vertical effective stresses. Error bars represent +/- standard error, ϵ_b .

Comparison of b-Values from the Literature and Impact on MSF

Although it does not provide comprehensive coverage of every study on N_{eq} and MSF, this section presents b-values used in some recent and/or prominent studies for computing N_{eq} and/or MSF and compares them to the b-value recommended herein (i.e., b=0.28). The previous studies included in this comparison are Arango (1996) [A96], Idriss (1997) [I97], Liu et al. (2001) [Lea01], Boulanger and Idriss (2014) [BI14], and Green et al. (2019) [Gea19]. A brief summary of the bases for the b-values used in these studies is presented, but particular attention is given to BI14 because it is one of the most recent studies on the list and also because it is the only study on the list that proposes a D_r -dependent b-value.

Similar to the present study, Arango (1996) developed a b-value for a proposed MSF relationship based on energy principles. However, the Arango (1996) b-value was based on stored energy in a cycle of loading as opposed to dissipated energy in a cycle of loading. As a result, his derived b-value (i.e., b = 0.5) inherently assumes that the soil's response is constrained to the elastic range, which is inconsistent with the liquefaction phenomenon. I97 repeated the N_{eq} study performed by Seed et al. (1975) but used a b-value that he derived from cyclic triaxial test data from Yoshimi et al. (1984), b = 0.34. Based on an extensive review of published CDSS data (i.e., De Alba et al. 1976; Ishihara and Yamazaki 1980; Tatsuoka and Silver 1981; Boulanger and Seed 1995), Lea01 used b-values ranging from 0.33 to 0.39 for sand having $45\% \le D_r \le$ 70% to develop their N_{eq} relationship, with an approximate average value of b = 0.36. In addition, Lea01 also used the b-value derived by Arango (1996) (i.e., b = 0.5) in developing their N_{eq} relationship. From a limited parametric study using the IZ modulus reduction and damping (MRD) curves in conjunction with the dissipated energy approach detailed in this paper, Gea19 used b = 0.34 for their proposed MSF relationship. Because this value was consistent with the value used by I97 based on laboratory data, Gea19 did not perform a more extensive parametric study. Similar to the present study, all of these past studies proposed D_r -independent b-values; a comparison of these proposed b-values along with the value proposed herein is shown in Fig. 13. However, as detailed in the following, BI14 proposed a D_r -dependent b-value relationship.

BI14 proposed a new MSF relationship as part of their revised stress-based liquefaction evaluation model, which entailed a D_r -dependent b-value relationship. BI14 assumed that motions for $M \leq 5.25$ can be reasonably represented by three-fourths cycles having amplitude $a_{\rm max}$. Per Eq. (1), $N_{\rm min}$ (i.e., N_{eq} for $M \leq 5.25$) for these motions can be computed as follows:

$$N_{\min} = \left(\frac{a_{\max}}{0.65 \cdot a_{\max}}\right)^{\frac{1}{b}} \cdot \frac{3}{4} = \left(\frac{1}{0.65}\right)^{\frac{1}{b}} \cdot \frac{3}{4}$$
 (8)

where b varies as a function of soil density as shown in Fig. 13; this was back-calculated from expressions given in Boulanger and Idriss (2014), and Eq. (7) was used to relate q_{c1Ncs} and D_r . However, based on a parametric analysis, BI14 determined the $N_{eqM7.5} \approx 15$ cycles, independent of D_r . Using these values of N_{\min} and $N_{eqM7.5}$ in conjunction with Eq. (2) for MSF and the b-value relationship shown in Fig. 13, BI14 developed an MSF relationship by interpolating/extrapolating in logarithmic space for other magnitude values. As a result, the dependency of the BI14 MSF relationship on soil density is most pronounced for $M \leq 5.25$ and inherently becomes less dependent on soil density as M approaches 7.5 (and is independent of soil density for M7.5).

To illustrate the effect on MSF of using a D_r -independent b-value versus a D_r -dependent b-value, the b-value recommended herein (i.e., b=0.28) and the b-value relationship proposed by BI14 (i.e., Fig. 13) were used to compute MSF for case histories in the BI14 CPT-based case history database. Because BI14 did not propose an N_{eq} relationship per se, the N_{eq} relationship proposed by Lasley et al. (2017) for shallow crustal events in active tectonic regimes (e.g., western US) was used in conjunction with Eq. (2) for MSF for this illustration:

$$N_{eq} = \exp[0.4605 - 0.4082 \log(a_{\text{max}}) + 0.2332M]$$
 (9)

Eq. (9) expresses N_{eq} as a function of M and a_{max} (in units of g). Based on a review of liquefaction case history databases, a_{max} for the reference M7.5 event was assumed to be 0.35g. This resulted in

 $N_{eq\,M7.5}=14$ cycles (Green et al. 2019). Therefore, Eq. (2) reduces to

$$MSF = \left(\frac{N_{eq}}{14}\right)^{-b} \tag{10}$$

The resulting MSF relationships are shown in Fig. 14. Per Eq. (9) the MSF varies as a function of a_{max} and M (i.e., MSF = 1 for M7.5 and $a_{\text{max}} = 0.35g$), and the effect of the b-value's dependency on D_r is noticeable. For example, when the D_r -dependent b-value is used, the MSF ranged from 1.09 to 1.21 for M6.0 and $a_{\rm max}=0.5g$ for $D_r=20\%$ to 80%. Also plotted in Fig. 14 are the MSFs for the liquefaction/no-liquefaction case histories in the BI14 CPT database, computed using both the D_r -independent and D_r -dependent b-values. Nearly all of the case histories were associated with $5.9 \le M \le 7.7$, and only one event was outside this range (2011 Tohoku, Japan: M9). In addition, the majority of the critical layers identified in this case history database had a D_r between 30% and 70%. Given this relatively confined range, the b-value D_r -dependency may seem to have a relatively minor impact when the resulting MSFs are compared directly, as shown in Fig. 15. However, for forward analyses cases where D_r , a_{max} , and/ or M approach their lower or upper extremes, such as evaluating liquefaction during induced events (e.g., Green et al. 2020), the difference between D_r -independent and D_r -dependent MSFs can be significant.

An important assumption inherent to Eq. (1) (for computing N_{eq} for earthquake ground motions) and to Eq. (2) (for MSF) is that the CSR versus N_L relationship is linear in log-log space. However, several studies show that this relationship is not always linear, or at least it is not linear over the full range of N_L (Mandokhail et al. 2017; Ulmer et al. 2018). This nonlinearity is particularly pronounced in denser soils compared to looser soils and in the lower N_L range and may skew the observed relationship between b-values and D_r , leading to the common assumption that b-values increase with increasing D_r . This, along with the dependency of b-values on the liquefaction triggering criterion and quality acceptance criteria in laboratory tests, provided an impetus to devise an alternative approach for determining the b-value. The merits of an

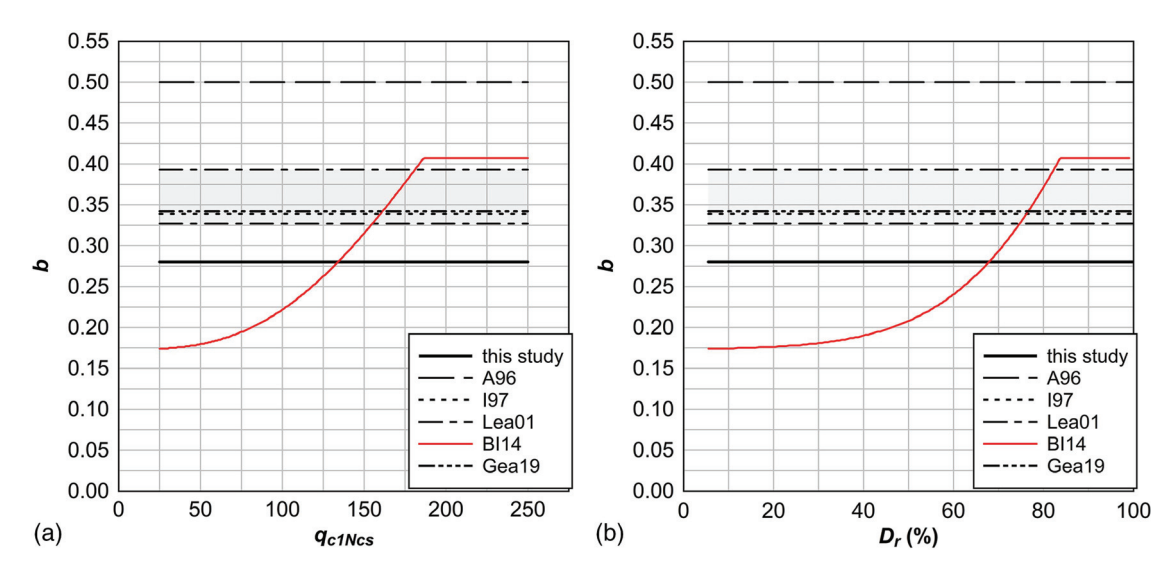


Fig. 13. Density-dependent b-value relationship derived from relationships given in Boulanger and Idriss (2014) for soil density quantified in terms of: (a) normalized CPT penetration resistance, q_{c1Ncs} ; and (b) D_r Also plotted are the b-values proposed herein and in previous studies. (A96: Arango 1996; I97: Idriss 1997; Lea01: Liu et al. 2001; BI14: Boulanger and Idriss 2014; Gea19: Green et al. 2019.)

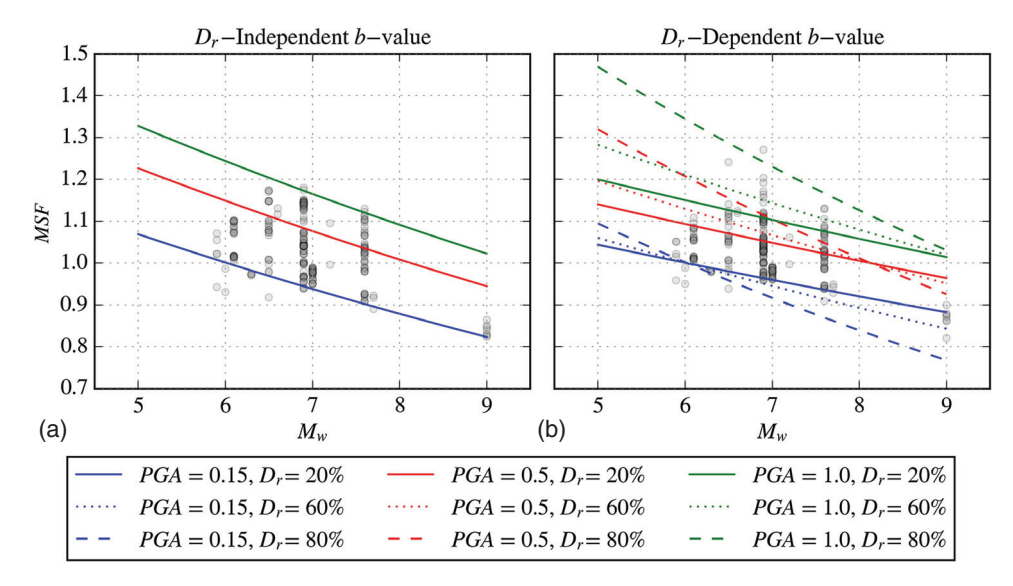


Fig. 14. MSF relationships using (a) D_r -independent b-value (this study, b = 0.28); and (b) D_r -dependent b-value (BI14). Gray circles represent values of MSF computed using the BI14 CPT-based case history database. Darker markers represent overlapping data points, and peak ground acceleration (PGA or a_{max}) values are in units of g. (Data from Boulanger and Idriss 2014.)

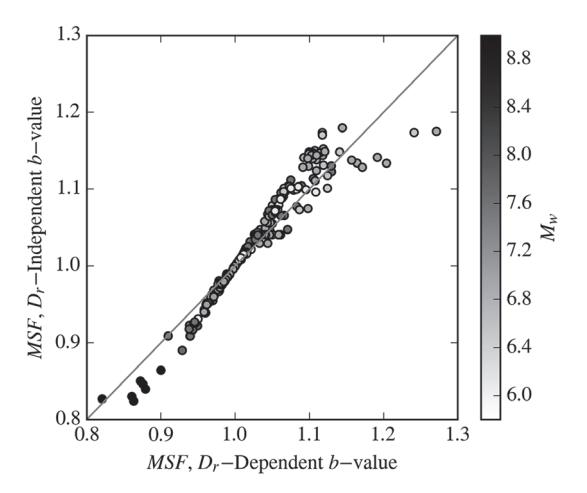


Fig. 15. Direct comparison of MSF values using D_r -independent b-value (this study, b = 0.28) and D_r -dependent b-value (BI14) for the liquefaction/no-liquefaction case histories in the BI14 CPT-based case history database. Darker marker edges represent overlapping data points. (Data from Boulanger and Idriss 2014.)

energy-based liquefaction criterion make it a compelling and appealing candidate for designating the initiation of liquefaction in laboratory tests and thereby defining b-values.

The energy-based criterion proposed herein is consistent with how N_{eq} is determined using fatigue theories (Green and Terri 2005) and correlates well with pore pressure generation (Green et al. 2000; Polito et al. 2008). In this study, the laboratory testing results showed that b-values derived from using $\Delta W_{\rm total}/\sigma'_{vo}=0.001$ as the liquefaction triggering criterion were relatively insensitive to changes in D_r and σ'_{vo} , which justifies the use of a constant b-value rather than a b-value that is a function of D_r and σ'_{vo} . The b-values based on MRD curves are computed using contours of constant ΔW , are also relatively insensitive to changes in D_r and σ'_{vo} , and represent a wider range of soils than b-values determined from cyclic laboratory tests performed on a single soil type or on a

few different soils. Therefore, b = 0.28 is recommended; this value was determined using the IZ MRD curves.

Although the recommended b-value of 0.28 is higher than the values obtained from the AC CV-CDSS tests using energy-based criteria and performed as part of this study (0.15–0.25), it is within the reasonable range of b-values from other studies (i.e., Fig. 13) and is consistent with b-values from a range of other soil types. A compilation of b-values computed from published cyclic laboratory tests, representing a range of confining stresses, soil types, liquefaction triggering criteria, and so forth, is shown in Fig. 16. Only b-values with $\epsilon_b \le 0.05$ were included in this figure. Results from CDSS tests yield b-values from 0.09 to 0.36, with an average of 0.21. Also shown in Fig. 16 are the inherent b-values backcalculated from a set of equations given by BI14 (same as in Fig. 13). The range of back-calculated b-values from the BI14 equations was approximately 0.19 ($D_r = 10\%$) to 0.41 ($D_r > 80\%$). The recommended b-value of 0.28 is an approximate average of this range. At first, it may appear that the BI14 equations fit the data better than the suggested b-value of 0.28, particularly for the CTRX tests. However, this is not the case for the CDSS tests, and CDSS tests are considered more representative of in situ ground responses due to vertically propagating shear waves. There is no discernable trend between b-values and D_r in CDSS tests as shown in Fig. 16; this supports the use of a single average b-value. Finally, the recommended b-value of 0.28 is within the range of the b-values from CDSS test data.

Summary and Conclusions

The objective of this study was to recommend a b-value(s) to compute N_{eq} and/or MSF as part of simplified, stress-based liquefaction triggering frameworks. Some of the conclusions drawn from this study are as follows:

1. An analysis in which b-values were computed using results of cyclic laboratory tests in the literature showed that b-values can be sensitive to many parameters, including soil type, sample preparation method, confining stress, liquefaction triggering criterion, and acceptance criteria in laboratory tests. The relationship between b-value and D_r is more ambiguous than

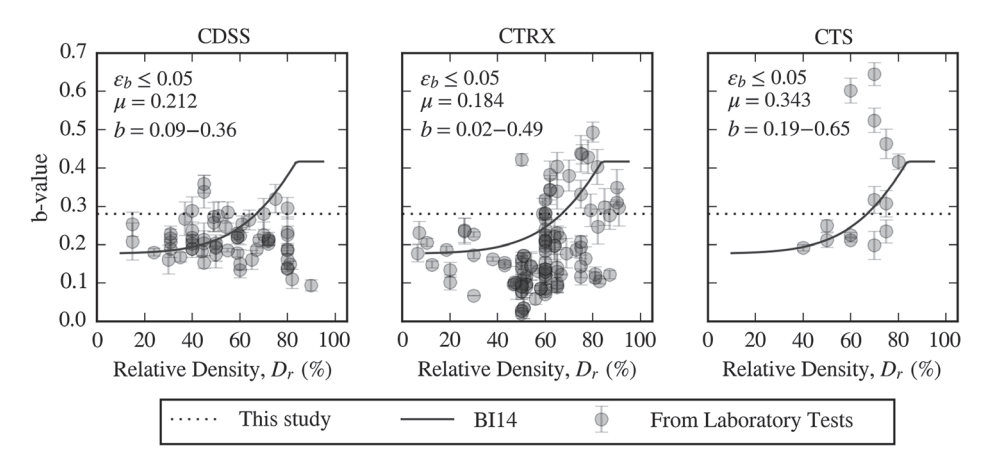


Fig. 16. Summary of *b*-values computed from published CDSS, CTRX, and CTS test results representing a range of soil types, confining pressures, and liquefaction triggering criteria. Darker marker edges represent overlapping data points. (Data for BI14 from Boulanger and Idriss 2014.)

previously assumed, likely due to interdependencies on secondary factors and/or nonlinearity in the log (CSR) versus log (N_L) relationship.

- 2. AC CV-CDSS tests performed as part of this study further emphasized the significance of quality acceptance criteria and liquefaction triggering criterion. The choice of liquefaction triggering criterion alone can have a significant effect on b-values, the standard error of b-values (ϵ_b), and the relationship (or lack thereof) between D_r and b-values.
- 3. An energy-based criterion for defining the CSR- N_L curves is mechanistically defensible for determining b-values because it is consistent with fatigue theories used to compute N_{eq} , and dissipated energy correlates well with excess pore pressure generation. Total normalized dissipated energy per unit volume of soil ($\Delta W_{\rm total}/\sigma'_{vo}$) is proposed as a liquefaction triggering criterion because the resulting b-values have lower uncertainty and are less sensitive to D_r and σ'_{vo} .
- 4. The b-values derived from MRD curves using $\Delta W_{M7.5}$ to define the liquefaction triggering criterion are reasonably independent of D_r and σ'_{vo} . Representative b-values for clean sands using the IZ and DS MRD curves are 0.28 and 0.20, respectively. These values and can be used to compute N_{eq} and MSF for evaluation of liquefaction triggering, although the authors give preference to the value of b=0.28 derived using the IZ MRD curves, because the IZ MRD curves are valid for the full range of shear strains of interest and have been shown to yield consistent trends with liquefaction test data (Green et al. 2022). Also, b=0.28 is more representative of laboratory derived b-values for varying soils, test conditions, and so forth.

Data Availability Statement

Some or all data, models, or code that support the findings of this paper are available from the corresponding author upon reasonable request.

Acknowledgments

The authors would like to thank Mr. Alex Osuchowski and Mr. Prakash Ghimire for their help in running the CV-CDSS tests and improving the testing procedures. This research was partially funded by the National Science Foundation (NSF) (Grant Nos. CMMI-1825189 and CMMI-1937984). This support is

gratefully acknowledged. However, any opinions, findings, and conclusions or recommendations expressed in this material are those of the authors and do not necessarily reflect the views of the NSF.

Supplemental Materials

Additional details about CV-CDSS testing, including Figs. S1–S3 and Tables S1 and S2, are available online in the ASCE Library (www.ascelibrary.org).

References

Arango, I. 1996. "Magnitude scaling factors for soil liquefaction evaluations." *J. Geotech. Eng.* 122 (11): 929–936. https://doi.org/10.1061/(ASCE)0733-9410(1996)122:11(929).

Boulanger, R. W., and I. M. Idriss. 2014. CPT and SPT based liquefaction triggering procedures. Rep. No. UCD/CGM-14/01. Davis, CA: Univ. of California.

Boulanger, R. W., and I. M. Idriss. 2015. "Magnitude scaling factors in liquefaction triggering procedures." *Soil Dyn. Earthquake Eng.* 79 (Dec): 296–303. https://doi.org/10.1016/j.soildyn.2015.01.004.

Boulanger, R. W., and R. B. Seed. 1995. "Liquefaction of sand under bidirectional monotonic and cyclic loading." *J. Geotech. Eng.* 121 (12): 870–878. https://doi.org/10.1061/(ASCE)0733-9410(1995)121:12(870).

Casagrande, A. 1976. Liquefaction and cyclic deformation of sands: A critical review. Harvard soil mechanics series No. 88. Boston: Harvard Univ.

Darendeli, M. B. 2001. "Development of a new family of normalized modulus reduction and material damping curves." Ph.D. dissertation, Dept. of Civil, Architectural, and Environmental Engineering, Univ. of Texas at Austin.

De Alba, P., H. B. Seed, and C. K. Chan. 1976. "Sand liquefaction in large-scale simple shear tests." *J. Geotech. Eng. Div.* 102 (9): 909–927. https://doi.org/10.1061/AJGEB6.0000322.

El Mohtar, C. S. 2009. "Evaluation of the 5% double amplitude strain criterion." In Proc., 17th Int. Conf. on Soil Mechanics and Geotechnical Engineering: The Academia and Practice of Geotechnical Engineering, 80–83. London, UK: International Society for Soil Mechanics and Geotechnical Engineering.

Green, R. A. 2001. "Energy-based evaluation and remediation of liquefiable soils." Ph.D. dissertation, Dept. of Civil and Environmental Engineering, Virginia Tech.

Green, R. A., et al. 2020. "Liquefaction hazard in the Groningen region of the Netherlands due to induced seismicity." J. Geotech. Geoenviron.

- Eng. 146 (8): 04020068. https://doi.org/10.1061/(ASCE)GT.1943-5606 .0002286.
- Green, R. A., J. J. Bommer, A. Rodriguez-Marek, B. W. Maurer, P. J. Stafford, B. Edwards, P. P. Kruiver, G. de Lange, and J. van Elk. 2019. "Addressing limitations in existing 'simplified' liquefaction triggering evaluation procedures: Application to induced seismicity in the Groningen gas field." *Bull. Earthquake Eng.* 17 (8): 4539–4557. https://doi.org/10.1007/s10518-018-0489-3.
- Green, R. A., A. Bradshaw, and C. D. P. Baxter. 2022. "Accounting for intrinsic soil properties and state variables on liquefaction triggering in simplified procedures." *J. Geotech. Geoenviron. Eng.* 148 (7): 04022056. https://doi.org/10.1061/(ASCE)GT.1943-5606.0002823.
- Green, R. A., M. Cubrinovski, B. Cox, C. Wood, L. Wotherspoon, B. Bradley, and B. Maurer. 2014. "Select liquefaction case histories from the 2010-2011 Canterbury earthquake sequence." *Earthquake Spectra* 30 (1): 131–153. https://doi.org/10.1193/030713EQS066M.
- Green, R. A., J. K. Mitchell, and C. P. Polito. 2000. "An energy-based excess pore pressure generation model for cohesionless soils." In *Proc.*, *John Booker Memorial Symp.—Developments in Theoretical Geomechanics*, edited by D. W. Smith and J. P. Carter, 383–390. Rotterdam, Netherlands: A.A. Balkema.
- Green, R. A., and G. A. Terri. 2005. "Number of equivalent cycles concept for liquefaction evaluations—Revisited." J. Geotech. Geoenviron. Eng. 131 (4): 477–488. https://doi.org/10.1061/(ASCE)1090-0241(2005) 131:4(477).
- Hancock, J., and J. J. Bommer. 2005. "The effective number of cycles of earthquake ground motion." *Earthquake Eng. Struct. Dyn.* 34 (6): 637–664. https://doi.org/10.1002/eqe.437.
- Idriss, I. M. 1997. "Evaluation of liquefaction potential and consequences: Historical perspective and updated procedure." In *Presentation notes*, 3rd short course on evaluation and mitigation of earthquake induced liquefaction hazards. Washington, DC: Federal Government of the United States.
- Idriss, I. M., and R. W. Boulanger. 2008. Soil liquefaction during earth-quakes. Monograph MNO-12. Oakland, CA: Earthquake Engineering Research Institute.
- Ishibashi, I., and X. Zhang. 1993. "Unified dynamic shear moduli and damping ratios of sand and clay." Soils Found. 33 (1): 182–191. https://doi.org/10.3208/sandf1972.33.182.
- Ishihara, K., and F. Yamazaki. 1980. "Cyclic simple shear tests on saturated sand in multi-directional loading." Soils Found. 20 (1): 45–59. https:// doi.org/10.3208/sandf1972.20.45.
- Lasley, S. J., R. A. Green, and A. Rodriguez-Marek. 2017. "Number of equivalent stress cycles for liquefaction evaluations in active tectonic and stable continental regimes." J. Geotech. Geoenviron. Eng. 143 (4): 04016116. https://doi.org/10.1061/(ASCE)GT.1943-5606.0001629.
- Liu, A. H., J. P. Stewart, N. A. Abrahamson, and Y. Moriwaki. 2001. "Equivalent number of uniform stress cycles for soil liquefaction analysis." *J. Geotech. Geoenviron. Eng.* 127 (12): 1017–1026. https://doi.org/10.1061/(ASCE)1090-0241(2001)127:12(1017).
- Mandokhail, S. J., D. Park, and J.-K. Yoo. 2017. "Development of normalized liquefaction resistance curve for clean sands." *Bull. Earthquake Eng.* 15 (3): 907–929. https://doi.org/10.1007/s10518-016-0020-7.
- Moss, R. E. S., R. B. Seed, R. E. Kayen, J. P. Stewart, A. Der Kiureghian, and K. O. Cetin. 2006. "CPT-based probabilistic and deterministic assessment of in situ seismic soil liquefaction potential." *J. Geotech. Geoenviron. Eng.* 132 (8): 1032–1051. https://doi.org/10.1061/(ASCE) 1090-0241(2006)132:8(1032).
- Nemat-Nasser, S., and A. Shokooh. 1979. "A unified approach to densification and liquefaction of cohesionless sand in cyclic shearing." *Can. Geotech. J.* 16 (4): 659–678. https://doi.org/10.1139/t79-076.
- Polito, C. P., R. A. Green, and J. Lee. 2008. "Pore pressure generation models for sands and silty soils subjected to cyclic loading." J. Geotech.

- Geoenviron. Eng. 134 (10): 1490–1500. https://doi.org/10.1061/(ASCE)1090-0241(2008)134:10(1490).
- Salgado, R., R. W. Boulanger, and J. K. Mitchell. 1997a. "Lateral stress effects on CPT liquefaction resistance correlations." J. Geotech. Geoenviron. Eng. 123 (8): 726–735. https://doi.org/10.1061/(ASCE)1090-0241(1997)123:8(726).
- Salgado, R., J. K. Mitchell, and M. Jamiolkowski. 1997b. "Cavity expansion and penetration resistance in sands." J. Geotech. Geoenviron. Eng. 123 (4): 344–354. https://doi.org/10.1061/(ASCE)1090-0241(1997) 123:4(344).
- Seed, H. B., I. M. Idriss, F. Makdisi, and N. Banerjee. 1975. Representation of irregular stress time histories by equivalent uniform stress series in liquefaction analyses. EERC 75-29. Berkeley, CA: Earthquake Engineering Research Center, Univ. of California.
- Stafford, P. J., and J. J. Bommer. 2009. "Empirical equations for the prediction of the equivalent number of cycles of earthquake ground motion." Soil Dyn. Earthquake Eng. 29 (11–12): 1425–1436. https://doi.org/10.1016/j.soildyn.2009.05.001.
- Tatsuoka, F., K. Ochi, S. Fujii, and M. Okamoto. 1986. "Cyclic undrained triaxial and torsional shear strength of sands for different sample preparation methods." Soils Found. 26 (3): 23–41. https://doi.org/10.3208/sandf1972.26.3_23.
- Tatsuoka, F., and M. L. Silver. 1981. "Undrained stress-strain behavior of sand under irregular loading." Soils Found. 21 (1): 51–66. https://doi .org/10.3208/sandf1972.21.51.
- Toki, S., F. Tatsuoka, S. Miura, Y. Yoshimi, S. Yasuda, and Y. Makihara. 1986. "Cyclic undrained triaxial strength of sand by a cooperative test program." Soils Found. 26 (3): 117–128.
- Ulmer, K. J., R. A. Green, and A. Rodriguez-Marek. 2020. "A consistent correlation between V_s, SPT, and CPT metrics for use in liquefaction evaluation procedures." In *Geo-Congress 2020: Geotechnical Earth-quake Engineering and Special Topics*, Geotechnical Special Publication 318, edited by J. P. Hambleton, R. Makhnenko, and A. S. Budge, 132–140. Reston, VA: ASCE.
- Ulmer, K. J., R. A. Green, A. Rodriguez-Marek, and C. D. P. Baxter. 2019. "Quality assurance for cyclic direct simple shear tests for evaluating liquefaction triggering characteristics of cohesionless soils." In *Proc.*, 17th European Conf. on Soil Mechanics and Geotechnical Engineering. London, UK: International Society for Soil Mechanics and Geotechnical Engineering.
- Ulmer, K. J., S. Upadhyaya, R. A. Green, A. Rodriguez-Marek, P. J. Stafford, J. J. Bommer, and J. van Elk. 2018. "A critique of b-values used for computing magnitude scaling factors." In *Proc.*, *Geotechnical Earthquake Engineering and Soil Dynamics V, Slope Stability and Landslides, Laboratory Testing, and In Situ Testing, GSP 293*, 112–121. Reston, VA: ASCE.
- Vaid, Y. P., and D. Negussey. 1988. "Preparation of reconstituted sand specimens." In *Advanced triaxial testing of soil and rock, ASTM STP 977*, edited by R. T. Donaghe, R. C. Chaney, and M. L. Silver, 405–417. Philadelphia: ASTM.
- Viana Da Fonseca, A., M. Soares, and A. B. Fourie. 2015. "Cyclic DSS tests for the evaluation of stress densification effects in liquefaction assessment." Soil Dyn. Earthquake Eng. 75 (Aug): 98–111. https://doi.org/10.1016/j.soildyn.2015.03.016.
- Wu, J., A. M. Kammerer, M. F. Riemer, R. B. Seed, and J. M. Pestana. 2004. "Laboratory study of liquefaction triggering criteria." In *Proc.*, 13th World Conf. on Earthquake Engineering. Tokyo: International Association for Earthquake Engineering.
- Yoshimi, Y., K. Tokimatsu, O. Kaneko, and Y. Makihara. 1984. "Undrained cyclic shear strength of a dense Niigata sand." Soils Found. 24 (4): 131–145. https://doi.org/10.3208/sandf1972.24.4_131.